Effect of Post-extrusion Heat Treatment on Mechanical Property of Aluminum Alloy 2024 Tube Produced Using Shear Assisted Processing and Extrusion (ShAPE)

Md. Reza-E-Rabby, Tianhao Wang, Nathan Canfield, Daniel Graff, Timothy Roosendaal, and Scott Whalen

Abstract

The present work deals with the Shear Assisted Processing and Extrusion (ShAPE) of aluminum alloy 2024 tubes and mechanical property optimization via post-extrusion heat treatments (T3510 and T8510). The ShAPE process enables extruding AA2024 at an extrusion speed of 7.4 m/min and extrusion temperature of 480 °C, which is otherwise beyond the extrudability limit of this alloy using conventional extrusion techniques. The ultimate tensile strength reaches 466 MPa for ShAPE+T3510 condition and 503 MPa for ShAPE+T8510 condition, both of which exceed the corresponding ASTM/ASM (minimum/typical) values for the studied tube geometry. The yield strength reaches 382 MPa for ShAPE+T3510 condition and 481 MPa for ShAPE+T8510 condition, both of which surpass any reported values in the literature or the highest industrial values. In addition, the ductility of AA2024 tube fabricated from ShAPE+T3510 or ShAPE+T8510 are evidently improved by the grain size refinement, second phase refinement, and enhanced uniformity in second phase distribution due to the severe plastic deformation of ShAPE process.

Keywords

Shear Assisted Processing and Extrusions (ShAPE) • AA2024 • Heat treatment • T3510 • T8510 • Natural aging • Artificial aging

Md. Reza-E-Rabby (✉) · T. Wang · N. Canfield · D. Graff · T. Roosendaal · S. Whalen
Applied Materials and Manufacturing Group, Energy and Environment Directorate, Pacific Northwest National Laboratory, 902 Battelle Blvd, Richland, WA 99354, USA
e-mail: md.reza-e-rabby@pnnl.gov

Md. Reza-E-Rabby
Pacific Northwest National Laboratory, 902 Battelle Boulevard, P.O. Box 999, MSIN K2-03 Richland, WA 99354, USA

Introduction

In the pursuit of developing a substitute for Duralumin [1], ALCOA invented aluminum alloy AA2024-T3 in 1931 with improved yield strength and fatigue performance compared to Duralumin and their first generation aluminum alloy such as AA2017-T4 [2]. Because of its high specific strength, AA2024 became one of the most useful aerospace alloys applied to aircraft structures such as fuselage skin, wing tension member, rib, shear web, etc. [3]. AA2024 is now well developed and optimized in terms of heat treatment (temper heat treatment), chemistry, production method of extruded profiles and rolled sheets/plates, etc., to the extent that the mechanical properties have reached plateau as documented in standard handbooks [3, 4]. In addition, AA2024 is also rated as one of the most difficult-to-extrude aluminum alloys in the extrudability scale however, slightly less difficult than any precipitation hardened AA7XXX alloy and some work hardened AA5XXX alloys [5]. The maximum extrusion speed of AA2024 was reported as 3.5 m/min for a conventional extrusion technique [6, 7]. The incipient melting of the secondary hardening phases (S-Al_2CuMg) of AA2024 resulted in a surface tearing or cracking at an elevated temperature (well below the melting temperature of bulk material i.e., at 502 °C) due to high strain that limit the extrusion speed of this alloy [5, 8, 9].

The present study aims at increasing the extrusion speed of AA2024 using Shear Assisted Processing and Extrusions (ShAPE) [10] such that higher production rate of this alloy might be a cost-effective and competitive solution beyond just the aerospace applications, for example, commercial vehicles, high-speed passenger trains, etc. ShAPE technology has been successfully demonstrated on two types of Al alloys at the extremes of the extrudability scale (very easy vs. very difficult to extrude), that is, AA6063 [11] and AA7075 [12]. In this study, AA2024 is extruded at an extrusion speed of 7.4 m/min. It is also well established that post-extrusion cold working and natural/artificial aging of

D. Eskin (ed.), *Light Metals 2022*, The Minerals, Metals & Materials Series,
https://doi.org/10.1007/978-3-030-92529-1_42

AA2024 improves the extrusion parts by enhancing dispersion of strengthening precipitates S/S′ phase (Al_2CuMg) [3, 5, 13, 14]. Different heat treatment sequences are also applied in this study to enhance the mechanical properties of ShAPE-extruded AA2024 tubes. The material properties are compared with standard test results for relevant heat treatments/tempers. This study also reports on preliminary microstructural characterizations of the ShAPE-extruded AA2024 tubes.

Experimental Procedure

Materials

The cold finish round bar of AA2024-T351 aluminum alloys were **procured commercially** and employed in the ShAPE process as the starting billet material. **The as-received AA2024-T351 was tested in-house per ASTM E8** [15] **on an MTS 810 222 kN test frame to confirm the ultimate tensile strength, yield strength, and elongation as 471 ± 1 MPa, 363 ± 1 MPa, and 25%, respectively.** The chemical compositions of AA2024 are also listed in Table 1. The AA2024 cylindrical billets were machined to have feedstock dimensions as 31.8 mm outer diameter (OD), 10.1 mm inner diameter (ID), and a length of 102 mm.

ShAPE Process

The AA2024 tubes were extruded using one-of-its-kind ShAPE machine designed at the Pacific Northwest National Laboratory and built by BOND Technologies. The AA2024 billets were placed into the billet container (ID = 31.85 mm) and mandrel (diameter = 10 mm) assembly shown in Fig. 1. The rotating die head contains spiral groove to enhance plastic deformation and flow of materials as the die plunges into the AA2024 billet. The ID of the die is 12 mm and its clearance from the mandrel dictates the thickness of the ShAPE tube, 1 mm thick in this study. The die, container, and mandrel are made of H13 steel that were heat treated to austenitized temperature and quenched to achieve hardness >50 HRC. A K-type thermocouple was attached at about 0.5 mm from the die face at a radius of 15.9 mm to sense die temperature during ShAPE processing. It should be emphasized that this temperature measurement may not be interpreted as the exact temperature of the material being extruded. The maximum hydraulic ram speed of 360 mm/min was applied during ShAPE which resulted in an extrusion speed of 7.4 mm/min at the die exit for the studied extrusion ratio of 20.6:1. It has been reported in friction stir welding (FSW) literature [16, 17] that the maximum strength of the recrystallized zone may occur when processed temperature is ~480 °C. Several ShAPE trials were run at different rotational speeds (not reported here). It was found that 75 RPM provided the desired processing temperature (482 °C) for this study.

Post-extrusion Heat Treatment

Post-extrusion heat treatments were performed immediately after the extrusion to obtain T3510 and T8510 temper conditions [4, 13]. Table 2 summaries the heat treatment sequences for representative samples in this study. It should be noted here that the only difference between T3510 and T8510 tempers are applying natural aging and artificial aging respectively, after the stretching with 3.5% total strain (cold working). The heat treatment was performed in a Neytech Vulcan 3–550 multi-state programmable furnace with an ambient environment.

Mechanical Testing

Tensile testing of the ShAPE+T3510 and ShAPE+T8510 tubes was performed using an MTS312.21 servo hydraulic test frame with a 25 kN load cell at 5.1 mm/min cross head speed. At least four specimens of each category of the heat-treated samples were cut into 127 mm long sections and tested per ASTM B557-15 [18]. The gage length of tensile test specimen was 50 mm and an Epsilon non-contact optical extensometer was employed for the strain measurement.

Microstructural Characterization

The microstructures of the ShAPE+T3510 and ShAPE +T8510 tubes were investigated along the transverse and longitudinal sections. The samples were mounted in epoxy and sequentially ground and polished using standard SiC grit papers with the final polishing sequence with colloidal silica (0.05 μm) using vibratory polisher. The polished specimens were analyzed under the scanning electron microscopy

Table 1 Chemical compositions of AA2024

Element	Cu	Mg	Mn	Fe	Si	Zn	Ti	Cr	Al
Content (wt%)	3.8–4.9	1.2–1.8	0.3-0.09	0.5 max	0.5 max	0.25 max	0.15 max	0.1 max	Balance

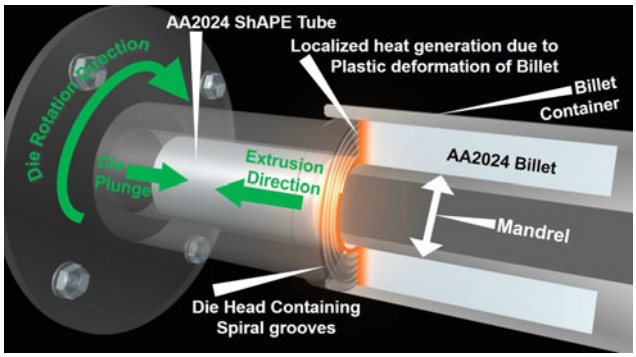

Fig. 1 ShAPE process and components for extruding AA2024 tubes

Table 2 Post-extrusion heat treatment of ShAPE-ed tubes [4, 13]

Sample ID	Temper designation	Heat treatment sequences
A	T3510	SHT* → WQ** → 3.5% cold working → NA***
B	T8510	SHT → WQ → 3.5% cold working → AA****

SHT* — Solution heat treatment at 495 °Cfor 1 h
WQ** — Water quench
NA*** — Natural aging for 30 days
AA**** — Artificial aging at 190 °C for 10 h

(SEM) for microstructural investigation. A JEOL 7001F FESEM with dual Bruker X-Flash 6|60 EDS detectors, Bruker e-Flash EBSD detector, and Esprit 2.1 software were used for chemical and microstructural evaluation of the samples. **The weighted average grain size of as-received AA2024 and ShAPE-extruded AA2024 was measured per ASTM E 1382–97** [19].

Results and Discussion

Tensile Strength of AA2024 Tubes

Figure 2 compares the ultimate tensile strength (UTS), 0.2% yield strength (YS) and % elongation at break of the AA2024 tubes produced using ShAPE followed by T3510 (white bars) and T8510 (gray bars) tempering. The relevant standard of ASM-typical, ASTM-minimum, and maximum reported industry values for the thin walled (<6 mm) tubes [3, 20, 21] are shown for comparison. The UTS of ShAPE + T3510 and ShAPE+T8510 are 467 ± 15 MPa and 523 ± 14 MPa (Fig. 2a). The average UTS values are increased by ~18% as compared with the ASM-typical and ASTM-minimum reported values and 0–8% higher than maximum reported industrial values for the corresponding temper conditions. Also, the 0.2% YS of ShAPE + T3510 and ShAPE + T8510 tempers are 380 ± 14 MPa and 496 ± 14 MPa, which far exceed ASM-typical and ASTM-minimum values (increased by ~30%, in Fig. 2b). Also these YS are about 17% and 11% higher than the maximum reported industrial values for corresponding T3510 and T8510 tempers. The elongation at break ShAPE + T3510 and ShAPE + T8510 tempers are ~100% higher than ASM-typical/ASTM-minimum values and on the par of industry values. An ongoing investigation will attempt to elaborately explain the underlying reason for this property improvement. However, following microstructural investigation will provide a glimpse on the relationship among the mechanical properties, grain structures, and distribution of strengthening precipitated of the ShAPE AA2024 tubes with respect to the base materials structures.

Grain Structures of Tubes from ShAPE + Post-Extrusion Heat Treatment

The pattern quality map of grain structures of as-received AA2024 bar and ShAPE+T3510 and ShAPE+T8510 AA2024 tubes in the longitudinal direction are presented in Fig. 3. The pancake-shaped elongated grain structure in Fig. 3a is commonly observed in the conventionally extruded AA2024 round bars. The minimum and maximum grain sizes in as-received AA2024 was measured from Fig. 3a as ~60 and ~190 µm, respectively, in the extrusion direction shown in Fig. 3d. The grains are significantly refined after the ShAPE plus post-extrusion heat treatment process (Fig. 3b–c). However, the trend of grain size refinement in the radial direction of ShAPE-extruded tubes possess different spreading between naturally aged (T3510) and artificially aged (T8510) AA2024 tubes. Table 3 summarizes the grain size variance through the wall thickness with 0 µm being the tube ID and the tube OD at about 1000 µm. Except the very few layers of grain near the ID of the tube, the grain growth occurred to some extent in artificially aged sample as presented the average grain size in Table 3.

Furthermore, Fig. 4 presents the pattern quality map of grain structures of as-received AA2024 bar and ShAPE +T3510 and ShAPE+T8510 AA2024 tubes in the transverse direction. The conventionally extruded AA2024 bar exhibited grain size within the range of 40–100 µm in the transverse direction (see Fig. 4a). The substantial grain refinement was observed after the ShAPE of AA2024 tubes with average grain sizes of 19.91 ± 9.16 µm and 26.57 ± 19.47 µm for respective tempering of T3510 and T8510 conditions. While the difference in grain size due to temper difference is statistically insignificant in the transverse direction, a phenomenon of grain growth as peripheral coarse grain (PCG) [22] along the edge of the tube OD was

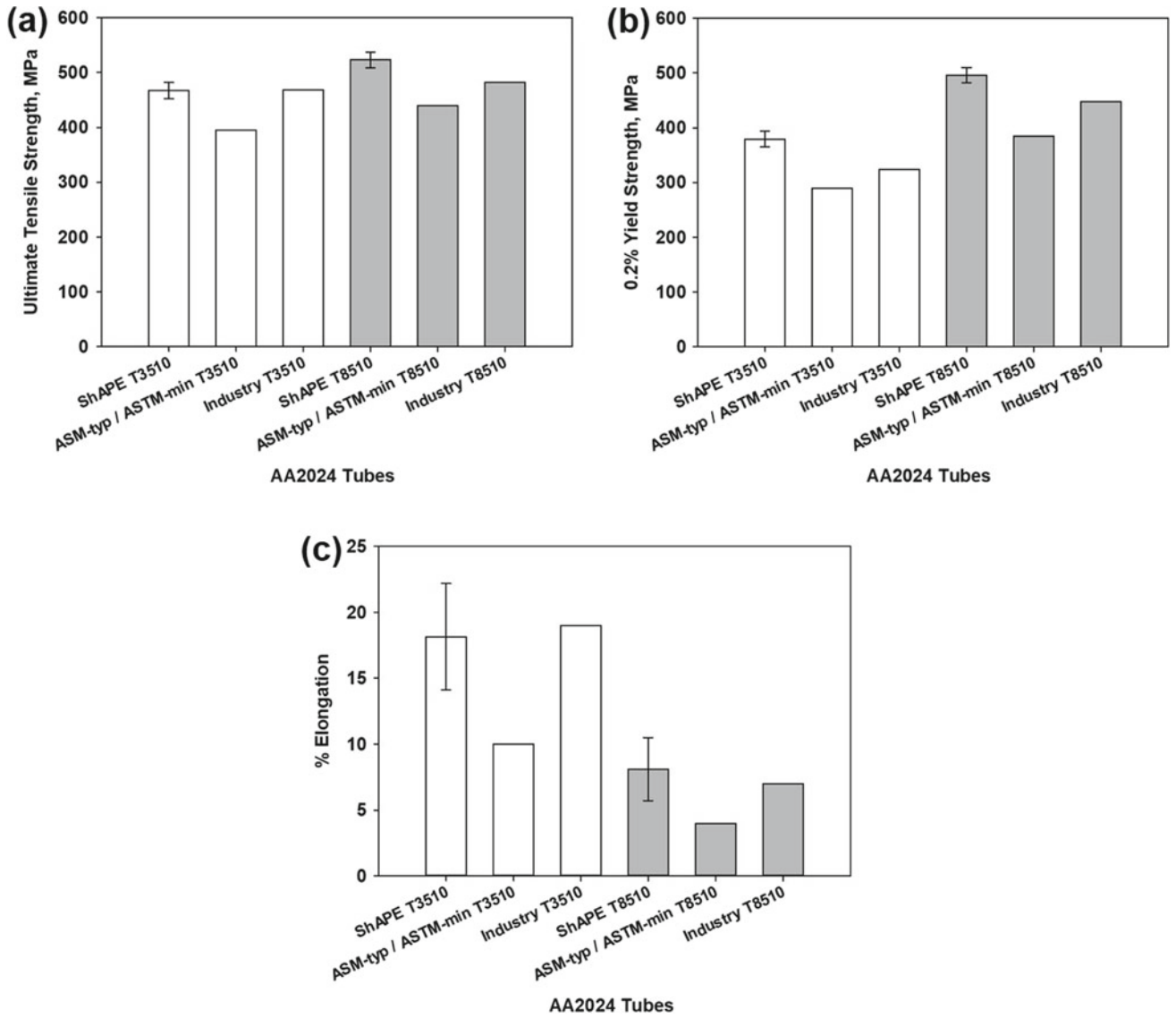

Fig. 2 Tensile properties of different tempered AA2024 tube and compared with relevant standard value [3, 20, 21]: **a** ultimate tensile strength, **b** 0.2% yield strength, and **c** % elongation

evident with artificial aging (T8510). In essence, the grain size refinement observed in both Figs. 3 and 4 is one of the contribution factors for improving the ductility (% elongation at break) of ShAPE-ed tubes with different post-extrusion heat treatments.

Strengthening Precipitation of ShAPE + Post-Extrusion Heat Treatment Tubes

Backscattered electron (BSE) SEM images of two tempered AA2024 ShAPE extruded tubes were evaluated to compare the secondary phase in Fig. 5a–b. The distribution of bright spots in low-magnification SEM micrographs of Fig. 5 a and b possess insignificant difference between naturally aged (T3510) and artificially aged (T8510) tubes. This phenomenon might attribute to the breakdown and uniform redistribution of secondary phases after the ShAPE process with the occurrence of trivial grain growth during artificial aging compared to natural aging. High-resolution SEM images with EDS mapping further reveal the precipitates distribution in which complex secondary phases of AlCuFeMeSi and AlCuFeMn were observed in addition to the presence of the principal hardening phase in the AA2024 system which are S (Al_2CuMg) and Ω (Al_2Cu) phases. Although, the cluster of S phase is commonly observed in both naturally and artificially aged samples, the dispersion of this phase was noticeable in AA2024-T8510 tube (Fig. 5b) compared to AA2024-T3510 tube (Fig. 5a) while comparing the Cu and Mg distributions. In addition, the T

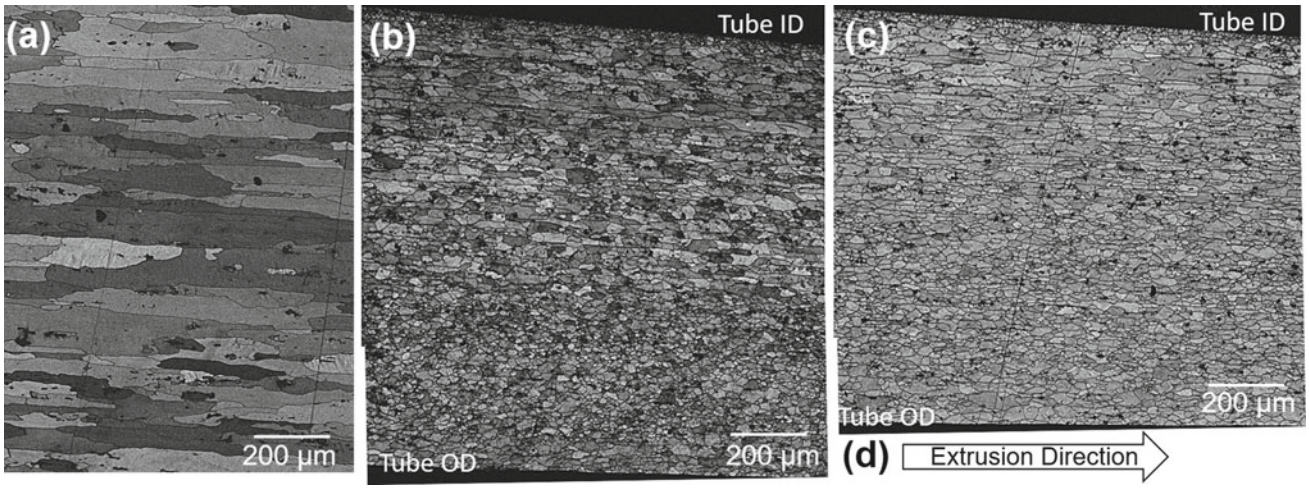

Fig. 3 Pattern quality map of grain structures of **a** as-received AA2024 extruded bar, **b** ShAPE + T3510, **c** ShAPE + T8510 tubes in longitudinal direction, and **d** extrusion direction

Table 3 Grain size measured along the radial direction of AA2024 tubes

ShAPE + different post-extrusion heat treatment	Radial distance with 0 being the edge of tube ID and full thickness ~1000 µm being the edge of tube OD			
	0–40 µm	40–640 µm	640–920 µm	920–1000 µm
T3510	10.5 µm	22.2 µm	17.1 µm	13.7 µm
T8510	8.77 µm	25.8 µm	20.8 µm	16.6 µm

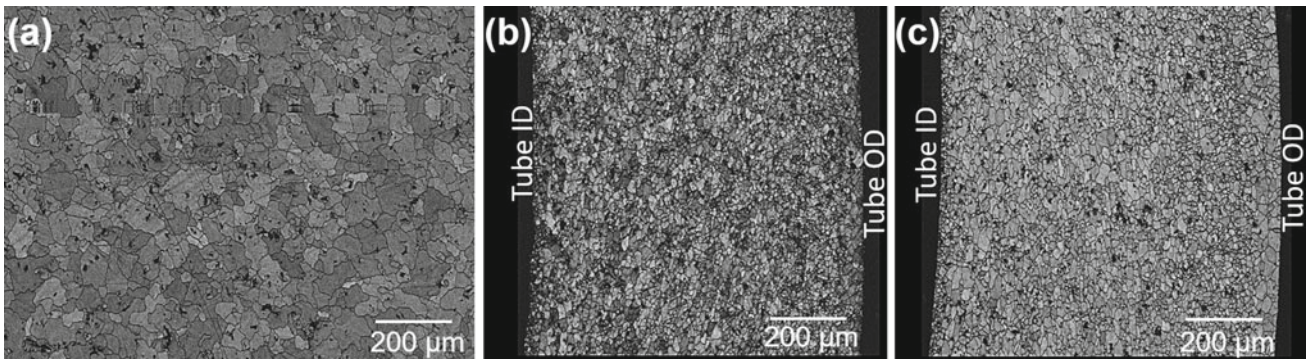

Fig. 4 Pattern quality map of grain structures of **a** as-received AA2024 extruded bar, **b** ShAPE + T3510 and **c** ShAPE + T8510 tubes in transverse direction

($Al_{20}Cu_2Mn_3$)-phase could not be precisely detected in the current study because of resolution limitations, however, might be estimated from the randomly distributed Mn element in both temper conditions (see Mn element mapping in Fig. 5a–b). Studies have shown that, these nano-sized T-phases formed during SHT and remain stable and assist nucleation of Ω-phase within it during the cold working and artificial aging [23–26]. It has also been reported that, both T- and Ω-phases activate the pinning and accumulation of dislocation during large plastic deformation and are responsible for improving the UTS and YS of AA2024-T8510 after artificial aging [16, 23–26]. This might also be true for ShAPE + T8510 condition in this study.

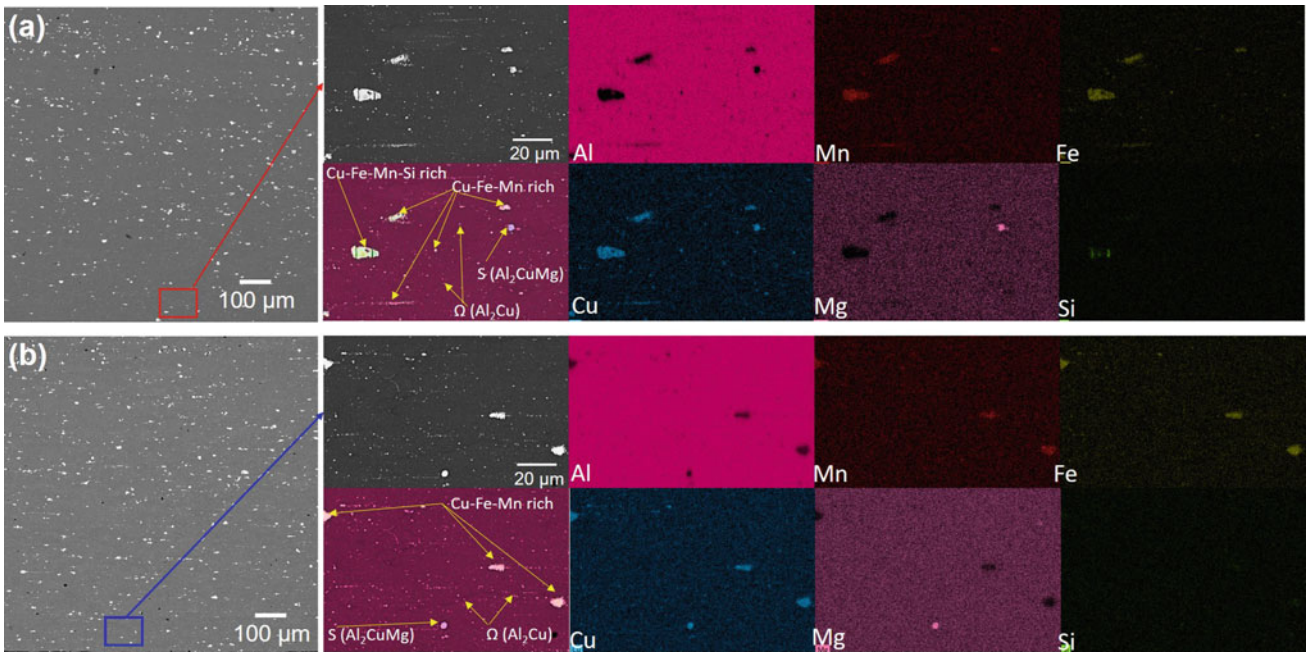

Fig. 5 SEM BSE images with EDS mapping illustrating the S phase in longitudinal sections of AA2024 ShAPE tubes after different post-extrusion heat treatment with **a** T3510 and **b** T8510 temper

Conclusions

The ShAPE has been demonstrated to produce 1 mm thick-walled AA2024 tubes at an extrusion speed of 7.4 m/min. This extrusion speed is twice that of otherwise commercially achievable speed of conventional extrusion processes. Moreover, the UTS, YS and % elongation of ShAPE-ed AA2024 are about 18, 30 and 100% higher than the ASM typical and ASTM minimum values for respective T3510 and T8510 conditions. In addition, the YS of ShAPE-extruded AA2024 are about 17% and 11% higher than the industry reported maximum values for the corresponding T3510 and T8510 temper. In essence, the ShAPE has enabled the refinement and re-distribution of second phases and strengthening precipitates at a faster extrusion speed with improved mechanical properties for precipitation-hardened AA2024 in this study.

Acknowledgements The Pacific Northwest National Laboratory is operated by the Battelle Memorial Institute for the United States Department of Energy under contract DE-AC06-76LO1830.The authors would like the acknowledge the support from the U.S. Department of Energy Advanced Manufacturing Office to conduct this work. The authors are also grateful for the dedication of Anthony Guzman for preparation of specimens for microstructural analysis.

References

1. O.H. Duparc, Alfred Wilm and the beginnings of Duralumin, Zeitschrift für Metallkunde, 96 (2005) 398-404.
2. R. Sanders, J. Staley, A History of Wrought Aluminum Alloys and Applications, in: K. Anderson, J. Weritz, J.G. Kaufman (Eds.) Properties and Selection of Aluminum Alloys, ASM International, 2019, pp. 162.
3. K. Anderson, J.G. Kaufman, J. Weritz, ASM Handbook: Volume 2B Properties and Selection of Aluminum Alloys, ASM International, 2019.
4. J.G. Kaufman, Introduction to Aluminum Alloys and Tempers, ASM International, 2013.
5. T. Sheppard, Extrusion of aluminium alloys, Springer Science & Business Media, 1999.
6. W.Z. Misiolek, R.M. Kelly, Extrusion of Aluminum Alloys, in: S. L. Semiatin (Ed.) Metalworking: Bulk Forming, ASM International, 2005, pp. 522–527.
7. P.K. Saha, Thermodynamics and tribology in aluminum extrusion, Wear, 218 (1998) 179–190.
8. M. Bauser, K. Siegert, Extrusion, ASM international, 2006.
9. T Sheppard, Extrusion of AA 2024 alloy, Materials science and technology, 9 (1993) 430–440.
10. C.A. Lavender, V.V. Joshi, G.J. Grant, S. Jana, S.A. Whalen, J.T. Darsell, N.R. Overman, System and process for formation of extrusion products, in, Google Patents, 2019.
11. B.S. Taysom, S. Whalen, M. Reza-E-Rabby, T. Skszek, M. DiCiano, Shear Assisted Processing and Extrusion of Thin-Walled AA6063 Tubing, in: Light Metals 2021: 50th Anniversary Edition, Springer International Publishing, 2021, pp. 281–285.

12. S. Whalen, M. Reza-E-Rabby, T. Wang, X. Ma, T. Roosendaal, D. Herling, N. Overman, B.S. Taysom, Shear Assisted Processing and Extrusion of Aluminum Alloy 7075 Tubing at High Speed, in: Light Metals 2021: 50th Anniversary Edition, Springer International Publishing, 2021, pp. 277–280.
13. D.S. MacKenzie, Heat Treatment Practice of Wrought Age-Hardenable Aluminum Alloys, in: K.F. Anderson, J. Weritz, J.G.F. Kaufman (Eds.) Aluminum Science and Technology, ASM International, 2018, pp. 462–477.
14. C. Zhu, K. Lv, B. Chen, On the S-phase precipitates in 2024 aluminum alloy: An atomic-scale investigation using high-angle annular dark-field scanning transmission electron microscopy, Journal of Materials Research, 35 (2020) 1582–1589.
15. ASTM E8 / E8M-21, Standard Test Methods for Tension Testing of Metallic Materials, in, ASTM International, West Conshohocken, PA, 2021.
16. C. Genevois, A. Deschamps, A. Denquin, B. Doisneau-Cottignies, Quantitative investigation of precipitation and mechanical behaviour for AA2024 friction stir welds, Acta Materialia, 53 (2005) 2447-2458.
17. Z. Zhang, B. Xiao, Z. Ma, Hardness recovery mechanism in the heat-affected zone during long-term natural aging and its influence on the mechanical properties and fracture behavior of friction stir welded 2024Al–T351 joints, Acta materialia, 73 (2014) 227-239.
18. ASTM B557–15, Standard Test Methods for Tension Testing Wrought and Cast Aluminum and Magnesium Alloy Products, in, ASTM International, West Conshohocken, PA, 2015, 2015.
19. ASTM E1382-97, Standard Test Methods for Determining Average Grain Size Using Semiautomatic and Automatic Image Analysis, in, ASTM International, West Conshohocken, PA, 2015, 2015.
20. ASTM B221-20, Standard Specification for Aluminum and Aluminum-Alloy Extruded Bars, Rods, Wire, Profiles, and Tubes, in, ASTM International, West Conshohocken, PA, 2020.
21. K. Aluminum, Tube and Pipe Alloy 2024 Technical Data Sheet, in, 2006.
22. A. Eivani, H. Jafarian, J. Zhou, Simulation of peripheral coarse grain structure during hot extrusion of AA7020 aluminum alloy, Journal of Manufacturing Processes, 57 (2020) 881-892.
23. Z. Feng, Y. Yang, B. Huang, M. Li, Y. Chen, J. Ru, Crystal substructures of the rotation-twinned T (Al20Cu2Mn3) phase in 2024 aluminum alloy, Journal of alloys and compounds, 583 (2014) 445–451.
24. M. Liang, L. Chen, G. Zhao, Y. Guo, Effects of solution treatment on the microstructure and mechanical properties of naturally aged EN AW 2024 Al alloy sheet, Journal of Alloys and Compounds, 824 (2020) 153943.
25. Z. Shen, C. Liu, Q. Ding, S. Wang, X. Wei, L. Chen, J. Li, Z. Zhang, The structure determination of Al20Cu2Mn3 by near atomic resolution chemical mapping, Journal of alloys and compounds, 601 (2014) 25–30.
26. Y.L. Zhao, Z.Q. Yang, Z. Zhang, G. Su, X. Ma, Double-peak age strengthening of cold-worked 2024 aluminum alloy, Acta Materialia, 61 (2013) 1624–1638.